LETTER • OPEN ACCESS

Unprecedented sea-ice minima enhances algal production deposited at the Arctic seafloor

View the article online for updates and enhancements.

ENVIRONMENTAL RESEARCH
LETTERS

LETTER

Unprecedented sea-ice minima enhances algal production deposited at the Arctic seafloor

Mark A Stevenson[1,3,*], Ruth L Airs[2] and Geoffrey D Abbott[1]

[1] School of Natural and Environmental Sciences, Newcastle University, Newcastle upon Tyne NE1 7RU, United Kingdom
[2] Plymouth Marine Laboratory, Plymouth PL1 3DH, United Kingdom
[3] Present address: Department of Geography, Durham University, Durham DH1 3LE, United Kingdom.
[*] Author to whom any correspondence should be addressed.

E-mail: mark.stevenson@durham.ac.uk

Abstract

Sea-ice in the Arctic is declining, with 2018 a particularly low year for ice extent, driven by anomalously warm atmospheric circulation in winter 2017/18. This is consistent with a multi-decadal trend to an earlier ice-free Barents Sea as climate change rapidly warms the Arctic. Here we investigate a N–S transect in the Barents Sea, crossing the Polar Front from Atlantic waters in the south to Arctic waters in the north, focusing on the organic geochemical signature (pigments and lipids) in surface sediments sampled in summer, between the years of 2017–19. Early ice-out in summer 2018 was confirmed by satellite imagery, tracking the evolution of Arctic sea-ice extent between years. Consistent with less extensive sea-ice cover in 2018 we found increases in multiple chlorophyll and carotenoid pigments as well as fatty acids (reflecting recent phytoplankton delivery) in the northern part of our transect at the seafloor. We attribute this to nutrient and organic matter release from earlier 2018 ice-out leading to stratification, post-melt phytoplankton blooms and the deposition of organic matter to the seafloor, evidenced by pigments and lipids. Organic matter delivered to the seafloor in 2018 was reactive and highly labile, confirming its deposition in the most recent season, pointing to rapid deposition. Correlations were found during ice-free periods between satellite-derived chlorophyll *a* and multiple indicators of water column productivity deposited at the seafloor. We also found convincing evidence of multi-year biogeochemical change across the Polar Front, where sedimentary change is marked by chlorophyll degradation products providing evidence of grazing, indicative of a tightly coupled ecosystem close to the marginal ice zone. Overall, our results show the tight coupling of Arctic productivity with the delivery and quality of organic matter to the seafloor and how this varies across the Barents Sea. More frequent early summer sea-ice loss driven by climate warming in the Barents Sea will have consequences for the delivery of organic matter to the seafloor with impacts for benthic organisms, microbiology and the sequestration of carbon.

1. Introduction

Climate change is leading to a longer ice-free period and earlier onset of sea-ice melt in the Arctic (Stroeve *et al* 2012, Notz and Stroeve 2016). This has consequences for ocean stratification, currents and temperature, which can shift the timing and abundance of primary productivity, altering the carbon and nutrient sources available to pelagic and benthic organisms (Kędra *et al* 2015, Post 2017). Sea-ice has a critical role in the regulation of the climate system and covers between 5% and 8% of the ocean surface (Comiso 2003), moderating feedback as ice has higher albedo than water (Wadhams 2000) and it helps maintain deep-water formation, vital to retain stratification in polar oceans (Bretones *et al* 2022). Since ~1980 increased inflow of Atlantic waters to the Barents Sea has contributed to warming of 1.4 °C (Stocker *et al*

2014), stimulating phytoplankton (Neukermans *et al* 2018). This is likely to be accelerated; modelling suggests the Barents Sea will be ice-free by 2050 with up to 4 °C of summer warming (Smedsrud *et al* 2013).

Satellite imagery has been used to detect and quantify reductions in Arctic sea-ice over decadal and sub-annual timescales (Serreze *et al* 2003, Comiso *et al* 2008), with sea-ice presence datasets available, based on satellite imagery at daily timescales (Spreen *et al* 2008). However, by solely looking at ice cover from space, it is difficult to ascertain the extent and timing of primary productivity changes taking place on the ice and in the water column and the effects of organic material on benthic productivity. Algal material and phytodetritus are key food sources for benthic animals (Boetius *et al* 2013) and microbial activity at the seafloor (Ravenschlag *et al* 1999, Orlova *et al* 2015), which ultimately mean that Arctic ocean sediments act as a carbon sink (Faust *et al* 2020, Stevenson *et al* 2020).

Phytoplankton and phototrophic bacteria are key sources of pigments to Arctic ocean sediments and have been used to understand phytoplankton communities, changes in primary production and alterations to the food web (Morata and Renaud 2008). The analysis of fatty acids and *n*-alkanes have been used to assess the quality of Arctic sedimentary organic carbon linked to marine productivity (Schubert and Stein 1997). Sterols are effective indicators of phytoplankton; the susceptibility of these compounds to degradation aids understanding of diagenetic processes (Volkman 1986, Belicka *et al* 2002, Belt *et al* 2015). Together, these markers can help assess the source of organic matter, as well as its abundance, quality and composition at the time of sampling.

Summer 2018 was a low year for Arctic sea-ice extent (Sumata *et al* 2022), with the Barents Sea ice-free earlier than usual (Downes *et al* 2021, Sumata *et al* 2022). To the west of the Barents Sea, there was an unprecedented decline in Arctic sea-ice outflow in 2018 of less than 40% of the annual mean (average September to August) between 2000 and 2017, a result of anomalously warm atmospheric circulation in winter 2017/2018 (Sumata *et al* 2022). Other parts of the Arctic had similar trends, with very little winter ice formation in the Bering Sea in 2018 (Stabeno and Bell 2019, Siddon *et al* 2020). In the Barents Sea, oceanographic observational data confirmed summer 2018 as being ice-free (Downes *et al* 2021), with diluted Atlantic water found close to the surface during Autumn 2018, following a long ice-free period (Lundesgaard *et al* 2022). This trend is consistent with the general trend towards an earlier ice-free Barents Sea which is becoming more frequent (Onarheim and Årthun 2017).

The Barents Sea is also influenced by varying Arctic and Atlantic currents which structure the supply of nutrients, phytoplankton and dependent consumers in the water column and at the benthos.

The transect investigated in this study crosses the Polar Front where warmer Atlantic water from the southwest, meets cooler Arctic water from the north, maintaining water column stratification (Barton *et al* 2018). Although one source of organic matter to the water-column is direct from sea-ice algae when it melts, also of importance are ice-edge phytoplankton, which take advantage of stable nutrient-rich conditions adjacent to ice due to stratification (Syvertsen 1991, Boetius *et al* 2013). Under-ice phytoplankton blooms where ice thins and meltwater ponds develop enabling light penetration have also been noted (Arrigo *et al* 2012). Water-column phytoplankton blooms occur shortly after ice-out, typically linked with its timing (Strass and Nöthig 1996, Dong *et al* 2020). Here, we use measurements of pigments, fatty acids, sterols, *n*-alkanols and *n*-alkanes in surface sediments (0.5 cm depth), reflecting most recent deposits and benthos from a N–S transect in the Barents Sea, replicated in the summers of 2017, 2018 and 2019, investigating the effect of the 2018 unprecedented sea-ice minima on the quality and quantity of phototrophic derived carbon to the seafloor. Additionally, a N–S transect across the Polar Front provides the opportunity to explore phototrophic indicators of transition to help distinguish the signatures of Arctic versus Atlantic water productivity.

2. Methods

2.1. Study locations and sampling

Sediment cores were retrieved in the months of July and early August in the Barents Sea aboard the RRS James Clark Ross in 2017 (JR16006), 2018 (JR17007) and 2019 (JR18006), from seven stations to the east and south of Svalbard. Most of the sampled area (except in the vicinity of B03 and B13, table 1) is seasonally ice covered (maximum = April; minima = September) (Vinje and Kvambekk 1991). Although most of the ice is locally formed, there is also seasonally variable multi-year drift ice from the Kara and Laptev Seas (Pavlov *et al* 2004, Hop and Pavlova 2008, Tamelander *et al* 2009). Station B14 marks the mean position of the Polar Front which inflexes north due to the effect of Atlantic currents (Fossheim *et al* 2006, Oziel *et al* 2016). Sampling sites north of B14 mainly feature cooler Arctic water overlain by seasonally variable less saline meltwater. Warmer more saline Atlantic water enters the Barents Sea from both the north (after circulating clockwise around Svalbard with the West Spitsbergen Current) and from the south (Loeng 1991, Sundfjord *et al* 2007).

Stations B13 to B17 reflect the primary 30 °E longitudinal transect across the continental shelf (average depth 287–359 m below sea level (mbsl)), with station B18 included as a deeper continental shelf-edge comparison (average depth 3001 mbsl).

Sediments from the southern Barents Sea at station B03 (72.6 °N, 19.3 °E; average depth 367 mbsl) enable comparison with Atlantic waters. Replicate measurements (displayed as standard deviations to indicate reproducibility) were obtained each year at stations through deployment of a multicorer three times within the same local area (within 50 × 50 m grid), except where ice floes prevented redeployment within the gird, extending grid area slightly. Due to ice thickness B18 was only sampled in 2017 and B17 in 2017/18. Cores were sectioned using a stainless-steel spatula into foil (pre-ashed) and frozen at −80 °C. Pigment samples remained frozen at −80 °C until analysis, biomarker samples were stored at −20 °C. Surface sediments for this study comprise the upper 0.5 cm of each core sampled.

2.2. Satellite imagery of sea-ice cover (SIC) and chlorophyll *a*

SIC was obtained from Pan-Arctic AMSR2 sea-ice concentration data at 3.125 km grid resolution (2017–2019) from Universität Bremen (https://seaice.uni-bremen.de/sea-ice-concentration) (Spreen *et al* 2008) based on publicly available data from GCOM-W1 satellite (https://gportal.jaxa.jp/gpr). Images were obtained to show seasonal sea-ice retreat from April to July across the Barents Sea (SI figure 1). SIC closest to sampling (table 1) is displayed in figure 1.

For sea-surface chlorophyll *a* in ice-free waters, OC-CCi v5.0 data (https://climate.esa.int/en/projects/ocean-colour/news-and-events/news/ocean-colour-version-50-data-release/) for the Barents Sea (2017–2019) was processed by NEODAAS (NERC Earth Observation Data Acquisition and Analysis Service www.neodaas.ac.uk/) (Sathyendranath *et al* 2019) for approximately monthly date ranges (May, June, July) corresponding to SIC data (SI figures 9–17). Chlorophyll *a* concentration was extracted from both 10 and 25 km^2 grids to highlight how spatial scales affect bloom dynamics (SI figures 6 and 7).

2.3. Total organic carbon (TOC)

TOC was determined on freeze-dried sediments acidified in porous crucibles (HCl; 4 M; 4 h), dried overnight (60 °C) and analysed with a CS230 carbon/sulphur determinator (Leco Corporation, St. Joseph, MI, USA), calibrated using standards. TOC values (SI. table 2) were used for correction of biomarker analyses.

2.4. Chlorophyll and carotenoid pigments

Surface sediments (2–3 g) were thawed and centrifuged (Eppendorf, 4000 rpm, 5 min, 4 °C) to remove excess water (Ward *et al* 2022), transferred to a pre-weighed extraction tube with 3 ml acetone (kept on ice), sonicated (Sonics Vibracell probe, 50 s, 40 W), left 1 h, centrifuged (Eppendorf, 4000 rpm, 5 min, 4 °C) and decanted (repeated until colourless).

Samples were filtered (0.2 μm, 17 mm Teflon syringe filters, DHI, Denmark) and injected onto an Agilent 1200 HPLC (Airs *et al* 2001) (Method C). Pigment extracts (80 μl) were mixed with MilliQ water (8 μl) in the autosampler (darkness at 4 °C) and injected onto the HPLC column (2 Waters Spherisorb ODS2 cartridges coupled together, each 150 × 4.6 mm, particle size 3 μm, protected with a precolumn containing the same phase). A mixed standard (DHI, Denmark) was analysed to check pigment resolution.

Chlorophyll and its degradation products were quantified according to response factors from standards (DHI, Denmark). For quantification of hydroxychlorophyllone (no standard available), the response factor for pheophorbide *a* was used as the two components have similar UV/vis absorbance spectra (Airs *et al* 2001). Selected sediment samples were analysed by LC/MS^n for assignment of components (Airs *et al* 2001). LC/MS^n was performed using an Agilent 6330 ion trap mass spectrometer via an atmospheric pressure chemical ionisation source (m/z 400–1100). Post column addition of acid was used to aid ionisation of metallated components (Airs and Keely 2000). Components were assigned based on relative retention time, on-line UV/vis spectra, protonated molecule and fragmentation data (Airs *et al* 2001). Pigments are expressed as μg g^{-1} TOC and listed with key ratios in SI table 1. Where possible, samples were analysed in triplicate at each station from separate multicore deployments (Error bars: ±1 SD). Measurements of pigments on surface sediments (0.5 cm) reflect primarily the most recent seasons deposition as the half-life of many labile pigments is approximately 3 weeks in Barents Sea sediments (Morata and Renaud 2008).

2.5. Organic biomarker analysis

Freeze-dried sediment (1.7–3.3 g) was spiked with internal standard (5α-androstane, known amount) and sonicated in dichloromethane (DCM):methanol (9:1 v/v) three times for 15 min (Stevenson *et al* 2020) based on Holtvoeth *et al* (2010). Following rotary evaporation the total lipid extract was left overnight in activated copper to remove sulphur and passed through an anhydrous sodium sulphate column using DCM. Dried extracts were transmethylated overnight using acetyl chloride in methanol (1:30 v/v) at 45 °C, with neutralisation of excess acids using a potassium carbonate column flushed with DCM. Derivitisation of compounds with hydroxyl groups (1 h, 65 °C) used N,O-bis(trimethylsilyl)trifluoroacetamide (BSTFA) (with 1% trimethylchlorosilane (TMS)).

1 μl aliquots in DCM were injected onto a 7890B gas chromatograph (GC) coupled to a 5977B MSD mass spectrometer (MS) (Agilent, Santa Clara, CA, USA) operated in full scan mode (70 eV; source temp 230 °C; helium flow 1 ml min). A 60 m HP1-ms fused silica capillary column (0.25 mm × 0.25 μm) (J&W

Scientific, Folsom, CA, USA) was used for separation with a gradient of $6\,°C\,min^{-1}$ to $17\,°C$, followed by a hold of 1 min and then a slower ramp of $2.5\,°C\,min^{-1}$ to $315\,°C$ and a final hold of 22 min. Retention time and mass spectra were used to identify organic compounds and quantification was relative to the peak area of 5α-androstane (internal standard, assumption of linear response). Error estimations are the result of relative percentage standard deviation calculations of a sample analysed in triplicate, applied on a percentage basis. Selected fatty acid methyl esters (FAMEs), *n*-alkanols, *n*-alkanes and sterols and ratios used in the study are listed in SI table 1.

3. Results

3.1. Comparing sea-ice and satellite-derived chlorophyll a cover in the Barents Sea between 2017, 2018 and 2019

Summer SIC was less extensive in July 2018 compared with July 2017 and 2019 (figure 1). In July 2017 there was a broken array of moderate-low concentration SIC between station B15 and B16, with higher concentration SIC (up to 90%) in the vicinity of stations B17 and B18 (figure 1(a)). In contrast, in July 2018 the sea-ice margin was north of B18 (82 °N) and ranged between 60% and 90% SIC (figure 1(b)). Thickest and most extensive SIC was in July 2019 when 90% SIC approached station B15, extending eastwards towards Svalbard and northwards to the Nansen Basin (figure 1(c)).

In 2017 SIC evolved from covering as far south as station B14 at 31 May 2017, with only a broken array of moderate-thin SIC present between B15 and B16 by 31 July 2017 (SI figure 1(a)), evidencing a northwards retreat scenario (table 1). In 2018 SIC extended as far as B14 at 30 April 2018. However, due to low SIC north and north–east of Svalbard and associated weather conditions, SIC was less fixed and became more mobile enabling extensive break-up by 31 May 2018, except for localised cover in the proximity of B16 (SI figure 1(b)). Subsequently, by 30 June 2018 all stations were free of SIC, meaning all sampling was conducted in ice-free conditions, as confirmed by SIC at 21 July 2018 (SI figure 1(b); table 1). In 2019 SIC retreat was less dynamic with extensive thick (>90%) extent as far south as B15 at 31 May 2019, which despite thinning (∼60%–80%) between B14 and B15 by 30 June 2019, became more consolidated north of B15 by 14 July 2019 due to weather conditions (SI figure 1(c)). Therefore, 2019 had extensive SIC during sampling (table 1).

Satellite-derived chlorophyll *a* during ice-free periods was noticeably higher in concentration and earlier in timing in the Barents Sea during 2018, spanning the full transect by May/June compared with only partial cover in 2017 & 2019.
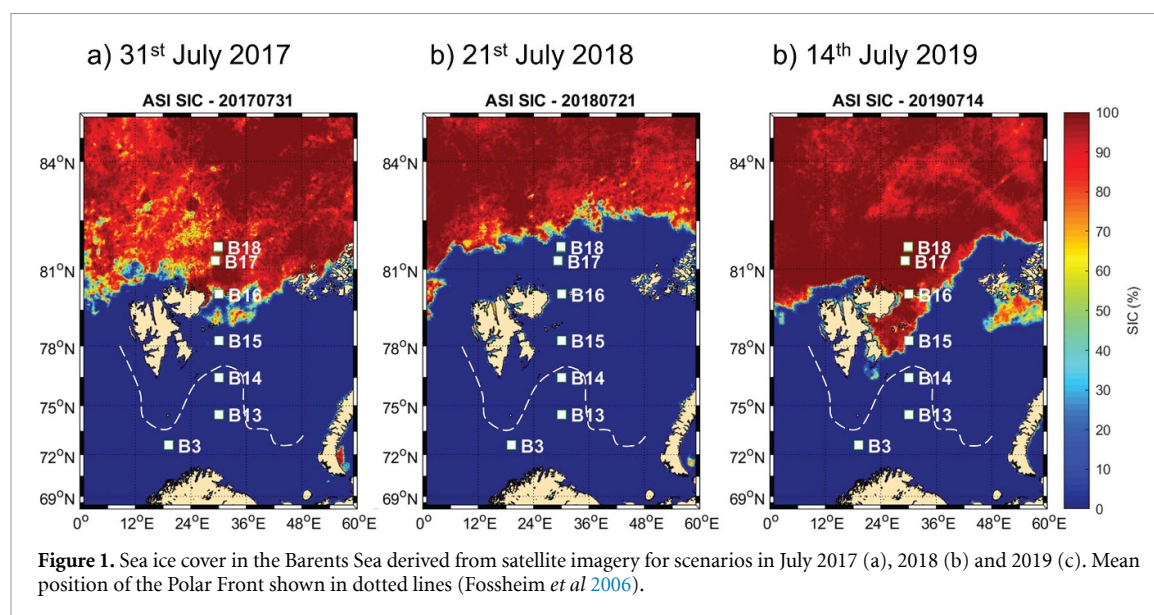
3.2. Indicators of algal production

Algal production was marked by consistently higher concentrations of pigments in 2018 at stations B16 and B17 when the northern Barents Sea was ice-free. Total chlorins were higher at B16 in 2018 (885 $\mu g\,g^{-1}$ TOC) compared with five- and eight-fold lower amounts in 2017 and 2019 (185 and 109 $\mu g\,g^{-1}$ TOC respectively) (figure 2(a)). At B17 chlorins were on average 20-fold higher in 2018 compared with 2017 (average of 5119 $\mu g\,g^{-1}$ TOC, compared with 253 $\mu g\,g^{-1}$ TOC respectively) (figure 2(a)). Trends were reflected by changes in key pigments such as chlorophyll *a*, hydroxychlorophyll *a* and fucoxanthin (figures 2(b)–(d)) and additional indicators in SI figures 2(a)–(c).

There was a marked but smaller secondary maxima in total chlorins around station B14 (averages 800 $\mu g\,g^{-1}$ TOC in 2017, 762 $\mu g\,g^{-1}$ TOC in 2018, 962 $\mu g\,g^{-1}$ TOC in 2019, figure 2(a)), in proximity with the mean position of the Polar Front (Fossheim *et al* 2006, Oziel *et al* 2016), which were consistently between stations B14 and B15 during sampling (SI figure 18). Similar trends were observed in chlorophyll *a* (figure 2(b)), fucoxanthin (figure 2(d)) and additional indicators in SI figure 2(a)–(c). The general position of the benthic Polar Front providing evidence of water mass separation between stations B14 and B15 was confirmed to be stable from bottom-water temperature versus salinity plots across all years (SI figure 18). Bottom water temperature at B15 in 2018 was slightly higher than 2017/19, when the Barents Sea was seasonally ice-free earlier than usual.

3.3. Indicators of fresh algal material

Both total FAMEs and summed short-chain (C_{14}, C_{16} and C_{18}) FAMEs were markedly higher in 2018 ice-free season compared with 2017 and 2019 ice-abundant seasons at stations B15–B17 (figures 3(a) and (b)), with 2018 concentrations rising consistently from station B03 to B17. Short chain FAMEs at B17 were more than four-fold higher in 2018 (average 7683 $\mu g\,g^{-1}$ TOC) compared with 2017 (average 1681 $\mu g\,g^{-1}$ TOC). Unaltered chlorophyll *a* ((chlorophyll *a*/identified chlorins) * 100) was also higher in 2018 reaching 43% at station B16 (compared with 14% in 2017 and 2019) and 60% at station B17 (compared with 25% in 2019) (figure 3(c)). The ratio of sterols campesterol/campestanol was also significantly higher in 2018 at stations B16 and B17, with a 15-fold difference at B17 between 2018 (ratio of 35) and 2019 (ratio of 2.3) (figure 3(d)). High fatty acid *n*-$C_{14/16}$ ratios were present in 2018 at stations B15 to B17 compared with 2017 and 2019 sampling (figure 3(e)), whereas the autochthonous/allochthonous ratio of FAMEs was most clearly elevated in 2018 at station B17 (ratio 27) compared with 2019 (ratio of 12) (figure 3(f)).

Figure 1. Sea ice cover in the Barents Sea derived from satellite imagery for scenarios in July 2017 (a), 2018 (b) and 2019 (c). Mean position of the Polar Front shown in dotted lines (Fossheim *et al* 2006).

Table 1. Locations of stations, depth to seafloor and date of samples used in this study.

Station	Average coordinates		Depth (m)		Date of sampling		
	Latitude °N	Longitude °E	Average depth	STDEV depth	2017	2018	2019
B03	72.634 056	19.255 80	367	4.4	5 August 2017	11 July 2018	26 July 2019
B13	74.439 771	29.957 94	359	2.1	16 July 2017	14 July 2018	7 & 8 July 2019
B14	76.502 223	30.500 25	295	2.7	30 July 2017	25 July 2018	13 July 2019
B15	78.219 199	29.957 37	317	1.7	19 July 2017	17 July 2018	10 & 11 July 2019
B16	80.099 403	30.026 23	287	9.6	21 & 22 July 2017	23 July 2018	16 July 2019
B17	81.145 437	29.394 80	337	2.4	24 July 2017	19 July 2018	
B18	81.762 930	30.078 84	3001	53.0	26 July 2017		

There were marked secondary increases in 2019 at station B14 in total FAMEs, short chain (C_{14}, C_{16} and C_{18}) FAMEs and % unaltered chlorophyll *a* (figures 3(a)–(c)) close to the Polar Front (Fossheim *et al* 2006), which was between B14 and B15 during sampling (SI figure 18). Complicating trends, in 2019 the ratio of campesterol/campestanol was highest at B03 and the fatty acid *n*-$C_{14/16}$ ratio was highest at B13 (figures 3(d) and (e)).
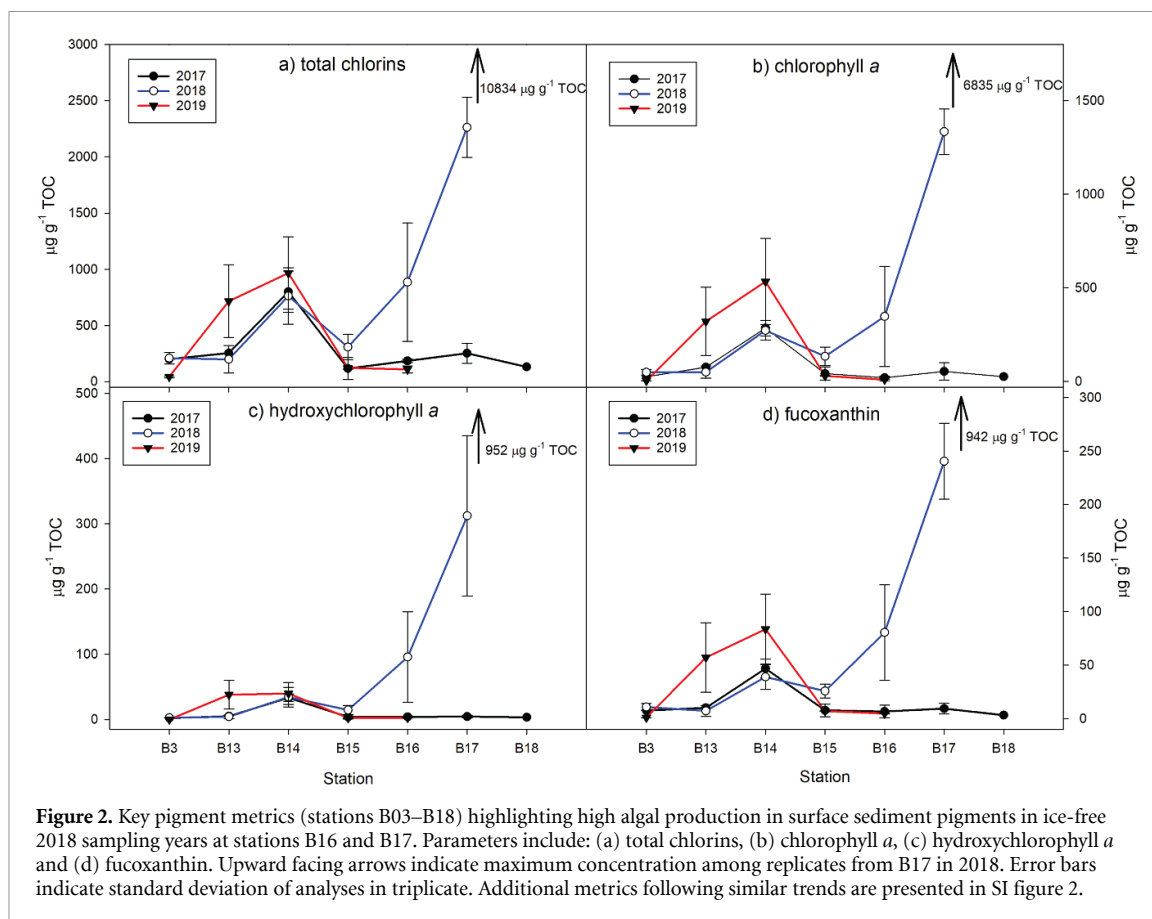
3.4. Indicators of transition across the Polar Front

A number of pigments and alteration products were especially good indicators of changes in primary producer community and variations in degradative susceptibility across the Polar Front, evidenced between B14 and B15 (Fossheim *et al* 2006) and from consistent benthic observations (salinity and temperature, SI figure 18). The carotenoid 19'-hexanoyloxyfucoxanthin was markedly higher in all three years at station B14 with averages ranging between 120 and 153 μg g^{-1} TOC, an ~50-fold increase from minima at B15 (~3 μg g^{-1} TOC) (figure 4(a)). Similarly, total carotenoids were also elevated (up to an average of 387 μg g^{-1} TOC) in 2017 at B14 (figure 4(b)), while continuing to show elevated concentrations at B16 and B17 in 2018. For pheophytin *b* and pyropheophytin *b* elevated

concentrations at B14 were most marked in 2017 (figure 4(c)), with highest hydroxychlorophyllone concentrations in 2017 and 2018 at B14 and 2019 at B13 (figure 4(d)).

3.5. Indicators of Arctic versus Atlantic water productivity

Differences between the southern-most stations and the main transect (B03 and B13) suggest differences in quality of organic matter in regions of Arctic versus Atlantic water productivity. Total sterols were six-fold higher at B03 compared with B13 in 2019 (6075 and 1011 μg g^{-1} TOC respectively), but in 2017 and 2018 there was no major difference (figure 5(a)). For the ratio of C_{14}, C_{15} and C_{16} iso FAMEs relative to *n*-$C_{16:0}$ FAME, values were higher in 2017 and 2018 in both B03 and B13 compared with B14-B17 but in 2019 it was only higher at B03 (figure 5(b)). C_{14}, C_{15} and C_{16} iso FAMEs relative to *n*-$C_{16:0}$ FAME was also markedly higher at the deeper shelf edge B18 site (when measured in 2018), in proximity to the northerly Atlantic influence around Svalbard. The ratio of dinosterol:dinostanol was significantly higher in 2017 at both B03 and B13, compared with B14-B18, but markedly higher only at B03 in 2019 (figure 5(c)). Stigmasterol:stigmastanol was higher at

Figure 2. Key pigment metrics (stations B03–B18) highlighting high algal production in surface sediment pigments in ice-free 2018 sampling years at stations B16 and B17. Parameters include: (a) total chlorins, (b) chlorophyll *a*, (c) hydroxychlorophyll *a* and (d) fucoxanthin. Upward facing arrows indicate maximum concentration among replicates from B17 in 2018. Error bars indicate standard deviation of analyses in triplicate. Additional metrics following similar trends are presented in SI figure 2.

B03 in all years compared with the B13 to B18 transect (figure 5(d)).

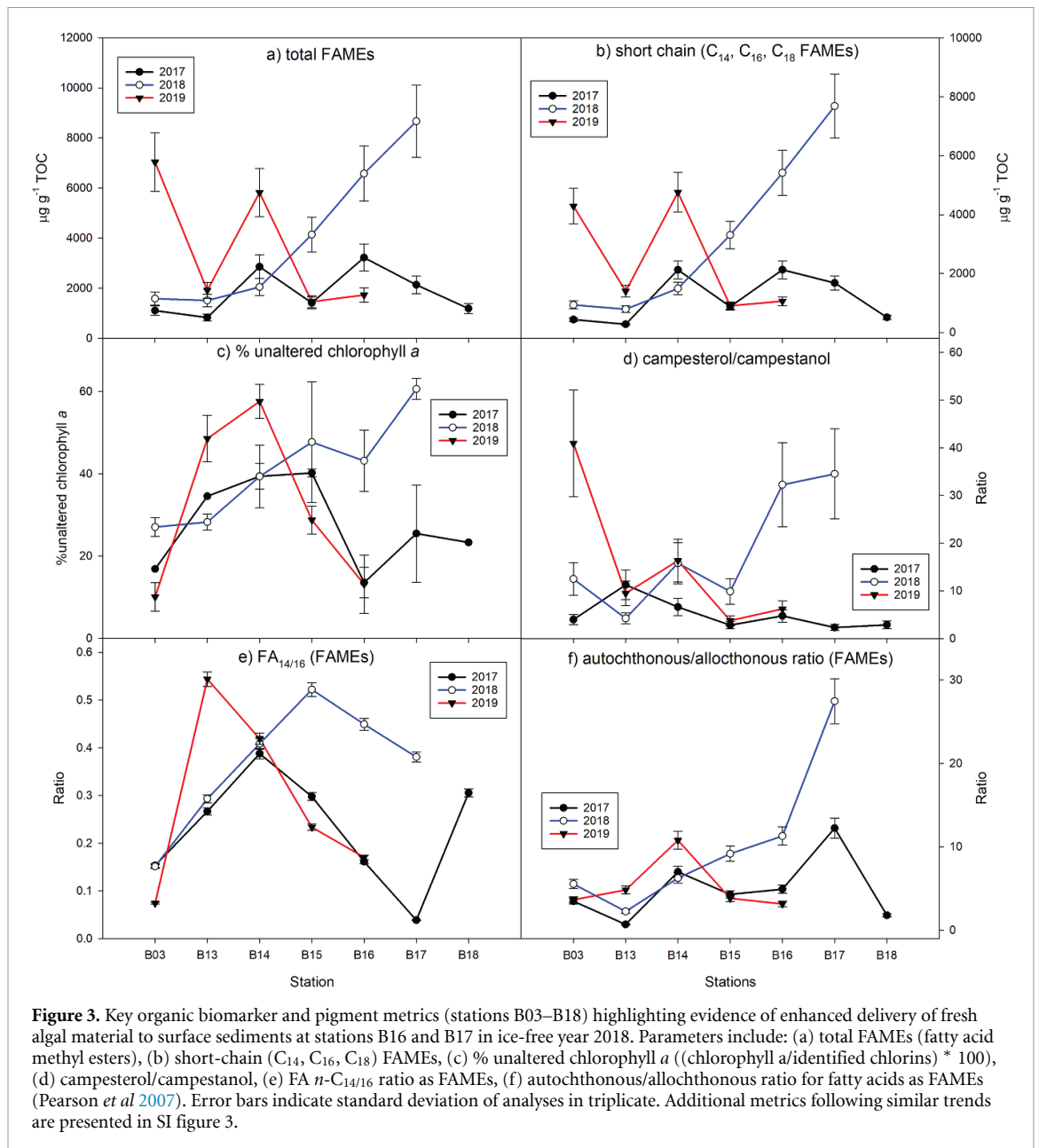### 3.6. Associations between indicators, samples and satellite-derived chlorophyll-*a*

Differences in 2018 ice-free sampling season at B16 and B17 highlighting high material quantity and quality are reflected in the upper-right part of the biplot (figure 6) and include total FAMEs, campesterol/campestanol, short-chain FAMEs, cholesterol/brassicasterol, % unidentified carotenoids, CPI_T FAMEs, FA short/long, fatty acid autochthonous/allochthonous, hydroxychlorophyll *a*/chlorophyll *a*, total SCEs and OEP_{17-21} *n*-alkanes (figure 6). In contrast, in the opposite part of the biplot variables are present which highlight differences between the southern part of the transect B03 and B13 compared with the rest of the transect (e.g. C_{14}, C_{15}, C_{16} iso/16:0 FAMEs and dinosterol/dinostanol) and complex relationships across the transect (e.g. pyropheophytin *a*/chlorophyll *a* and % unidentified chlorins). Variables such as short chain *n*-alkanols and total sterols are positioned midway between two groups and reflect variability at both parts of the transect.

Chlorophyll *a* concentration extracted from satellite imagery was markedly higher surrounding stations B17 and B18 in 2018 at a 25 km² resolution and higher also in 2018 surrounding stations B16, B17 and B18 at a 10 km² resolution (SI figure 6 &

7). There were good associations between satellite-derived chlorophyll *a* and in 2018 with chlorophyll *a*, diadinoxanthin, total chlorins, fucoxanthin, % unaltered chlorophyll *a* and short-chain FAMEs (SI figure 8).

4. Discussion

The markedly less extensive SIC in July 2018 (compared with 2017 & 2019) was contemporaneous with increases in multiple chlorophyll and carotenoid pigments at stations B16 and B17, indicating higher levels of photosynthetic production, characteristic of an extensive phytoplankton bloom. Mechanistically, this can be attributed to earlier nutrient release from ice-out and stratification, enabling extensive phytoplankton blooms and subsequent rapid vertical flux of chlorophylls and carotenoids to the seafloor. Shifts in the timing of primary productivity pulses may also generate a mismatch between pelagic grazers (e.g. copepods such as *Calanus* spp.) and their food sources (Ji *et al* 2013). Changes in surface sediment geochemistry, predominantly from fatty acids, sterols and pigment ratios (e.g. % unaltered chlorophyll *a*) at the same stations in 2018 provide insight into the delivery of fresh labile (more reactive) material to the seafloor in a summer of minimal SIC in the Barents Sea. Underlying the predominant 2018 increased production signature at the northerly

Figure 3. Key organic biomarker and pigment metrics (stations B03–B18) highlighting evidence of enhanced delivery of fresh algal material to surface sediments at stations B16 and B17 in ice-free year 2018. Parameters include: (a) total FAMEs (fatty acid methyl esters), (b) short-chain (C_{14}, C_{16}, C_{18}) FAMEs, (c) % unaltered chlorophyll *a* ((chlorophyll a/identified chlorins) * 100), (d) campesterol/campestanol, (e) FA n-$C_{14/16}$ ratio as FAMEs, (f) autochthonous/allochthonous ratio for fatty acids as FAMEs (Pearson *et al* 2007). Error bars indicate standard deviation of analyses in triplicate. Additional metrics following similar trends are presented in SI figure 3.
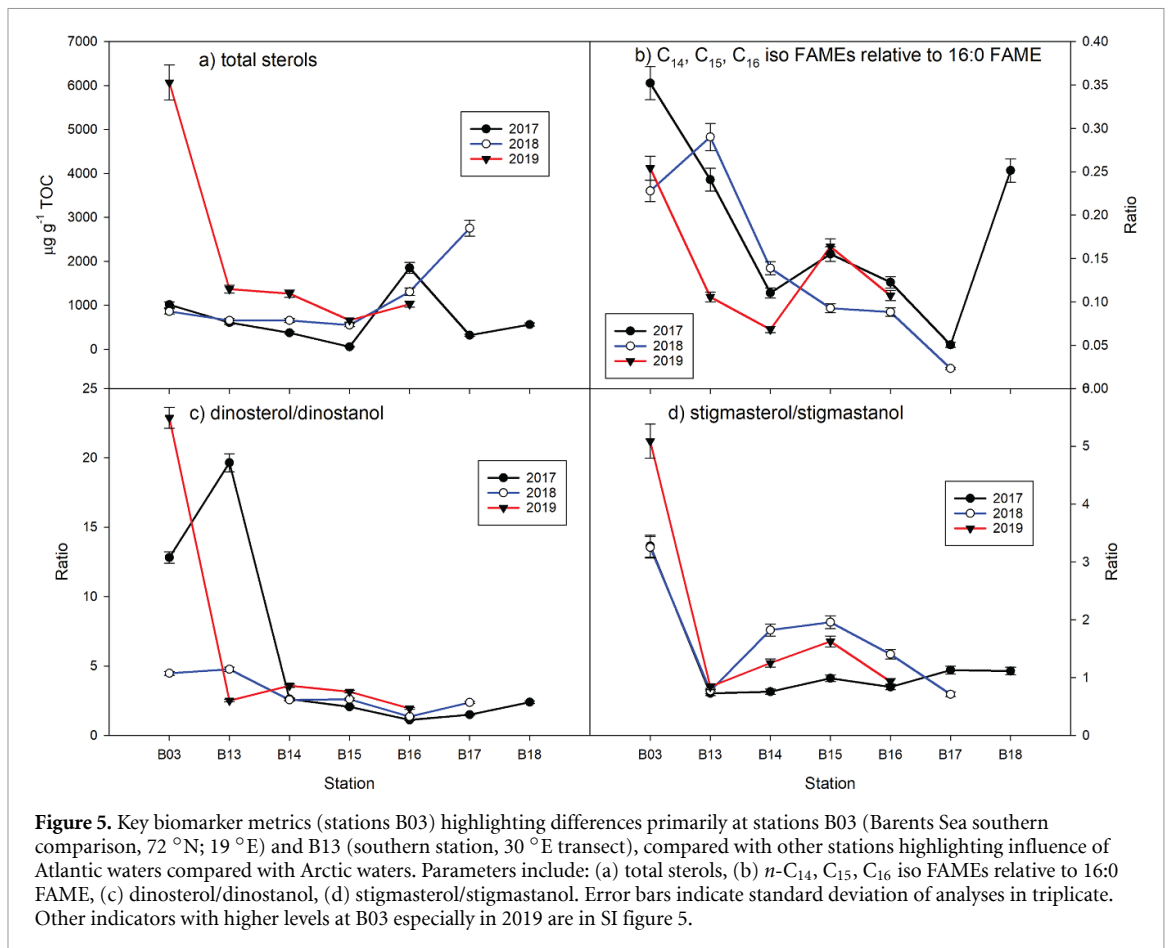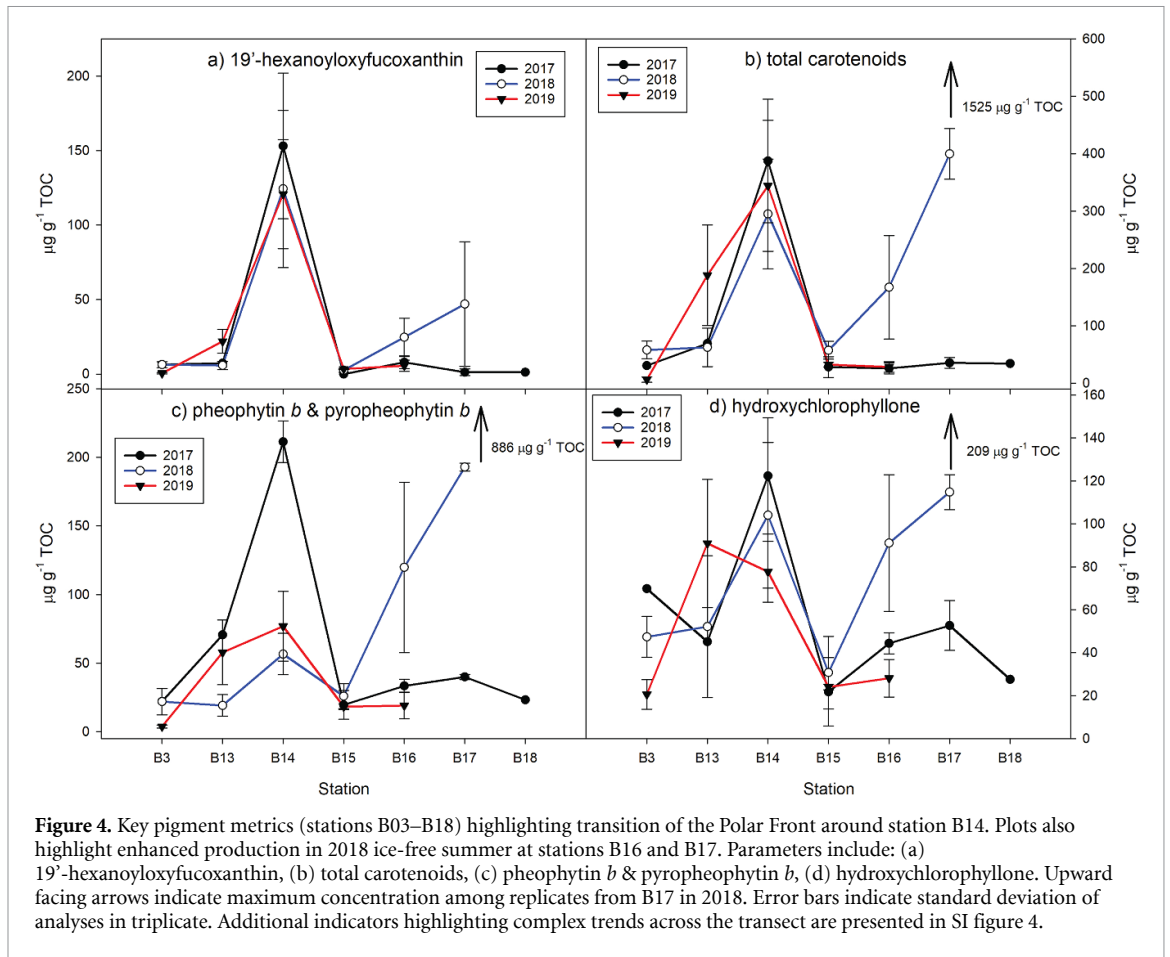
stations, additional geochemical parameters provide interpretable evidence in all years of complex fluctuations across the N–S transect, indicative of biological compositional changes in proximity to Atlantic and Arctic water masses and transitions across the Polar Front.
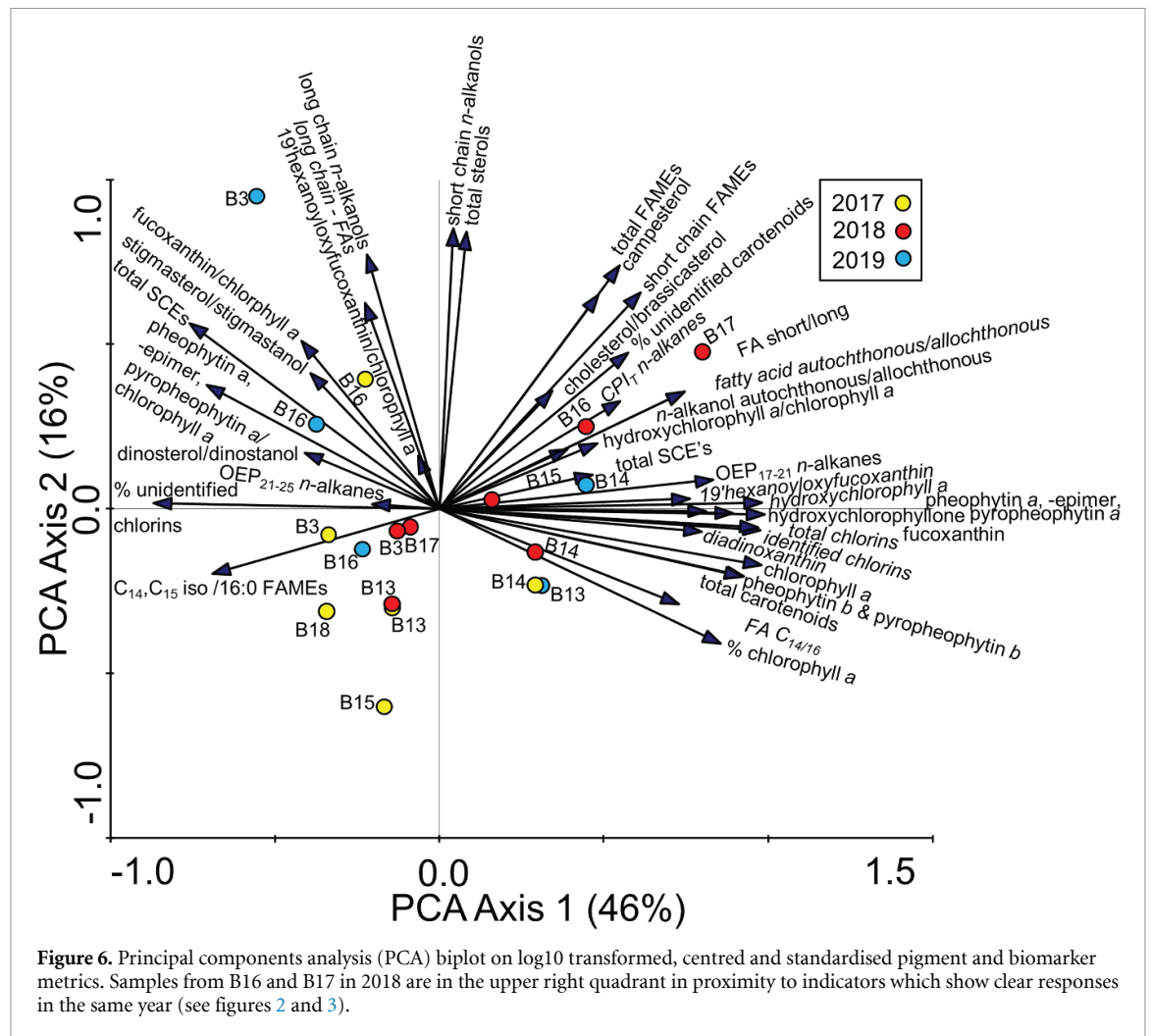
4.1. Increases in algal production in an ice-free Barents Sea

During the ice-free July 2018 high concentrations of multiple chlorophyll and carotenoid pigments (figure 2 and SI figure 2) at B16 and B17 can be explained by an early and extensive nutrient stimulated pelagic production response in this seasonally ice-covered part of the Barents Sea. Here, meltwater induces surface stratification where light and nutrient conditions enable phytoplankton growth (Fischer *et al* 2014, Dong *et al* 2020). The 2018 scenario of

an earlier and more productive ice-free Barents Sea is consistent with both an earlier onset of the high productivity season (on average 3.0 d yr^{-1} 1998–1995) (Kahru *et al* 2016) and also the trend to a more northerly and easterly expanse of spring and summer phytoplankton blooms (Oziel *et al* 2017). Close relationships between satellite derived chlorophyll *a* and multiple indicators of productivity measured at the seafloor (SI figure 8) demonstrate the link between pelagic phytoplankton blooms and material at the seafloor (Renaud *et al* 2008), which we interpret as the dominant source of organic matter delivery in the northern sector of the Barents Sea. Differences between satellite derived chlorophyll *a* at station B16 extracted at both the 25 km^2 and 10 km^2 grid sizes highlight how spatial scales affect bloom dynamics, which can be ephemeral (Dong *et al* 2020). A limitation is that satellite imagery cannot detect potential

Figure 4. Key pigment metrics (stations B03–B18) highlighting transition of the Polar Front around station B14. Plots also highlight enhanced production in 2018 ice-free summer at stations B16 and B17. Parameters include: (a) 19'-hexanoyloxyfucoxanthin, (b) total carotenoids, (c) pheophytin *b* & pyropheophytin *b*, (d) hydroxychlorophyllone. Upward facing arrows indicate maximum concentration among replicates from B17 in 2018. Error bars indicate standard deviation of analyses in triplicate. Additional indicators highlighting complex trends across the transect are presented in SI figure 4.

Figure 5. Key biomarker metrics (stations B03) highlighting differences primarily at stations B03 (Barents Sea southern comparison, 72 °N; 19 °E) and B13 (southern station, 30 °E transect), compared with other stations highlighting influence of Atlantic waters compared with Arctic waters. Parameters include: (a) total sterols, (b) *n*-C_{14}, C_{15}, C_{16} iso FAMEs relative to 16:0 FAME, (c) dinosterol/dinostanol, (d) stigmasterol/stigmastanol. Error bars indicate standard deviation of analyses in triplicate. Other indicators with higher levels at B03 especially in 2019 are in SI figure 5.

Figure 6. Principal components analysis (PCA) biplot on log10 transformed, centred and standardised pigment and biomarker metrics. Samples from B16 and B17 in 2018 are in the upper right quadrant in proximity to indicators which show clear responses in the same year (see figures 2 and 3).

benthic blooms (sampling stations ∼300 m.b.s.l.) and also the exact contribution from ice attached algae is challenging to disentangle (Boetius *et al* 2013).

Our observations are also consistent with phytoplankton extent, sea-ice and temperature trends in the northern Barents Sea which show more productive phytoplankton blooms in warm years (Dong *et al* 2020). Earlier ice retreat in the northern part of the Barents Sea in 2018 (see figure 1 and SI figure 1) may also reduce grazing pressure on phytoplankton resulting in greater vertical flux of pigments (and resulting carbon) to the seafloor (Renaud *et al* 2007), supported by a low proportion of steryl chlorin esters in 2018 (SI figure 5) and a high proportion of unaltered chlorophyll (figure 3(c)). Timing of the ice algal biomass peak in 2018 may also have been earlier (Ji *et al* 2013), although this may only partially explain the high algal production at B16 and B17 as sea-ice is known to typically contribute ∼20% of total primary production in the marginal sea-ice zone of the Barents Sea (Tamelander *et al* 2009).

The detection of multiple pigments at the sediment surface in 2018 at northerly stations B16 and B17 suggests a wide algal response with total chlorins,

chlorophyll *a* and its early derivative hydroxychlorophyll *a* (Walker *et al* 2002) all following similar increasing trends (figure 2). Pronounced increases in fucoxanthin and diadinoxanthin point to siliceous diatoms which are especially abundant in both under-ice phytoplankton blooms and at the ice-edge margin (Ardyna *et al* 2014). We know that the surface sediments deposited in summer 2018 are mostly related to recent events as the half-life of some labile pigments is approximately 3 weeks in polar sediments (Morata and Renaud 2008). In the marginal ice zone (north of station B15) due to the likely tight pelagic to benthic coupling (Tamelander *et al* 2006) we posit that around this location advection will be minimal compared with relatively local or sub-regional scale sedimentation of algal particles, which is supported by the Barents Sea being dominated by planktonic algae with small cells (Wassmann *et al* 2006). Additionally, it is known benthic sedimentary mixing is relatively slow and shallow from excellently preserved sediment cores in the region (Stevenson *et al* 2020, Faust *et al* 2021) and surface sediment radiocarbon dates on foraminifera have post-bomb ^{14}C ages (Faust *et al* 2023).

4.2. Evidence of highly reactive algal derived labile organic matter

Lipid signatures highlighted that delivery of organic matter in 2018, especially at stations B16 and B17 was fresh and highly labile (figure 3). Fatty acids are labile and susceptible to diagenesis, and so their higher abundance at the surface sediment under conditions of early ice retreat and bloom, support delivery of fresh phytoplankton material to the sediment surface. Fatty acids in sediments of the central Arctic have been linked to marine productivity (Schubert and Stein 1997) and are known to be high in both ice algae and phytoplankton in the Barents Sea marginal ice zone (Falk-Petersen *et al* 1998). High short-chain fatty acids could also result from the degraded remains of *Calanus sp.* which feed on phytoplankton blooms in the marginal ice zone of the Barents Sea (Falk-Petersen *et al* 2009). High percentage of unaltered chlorophyll *a* in 2018 also points to freshly deposited pigments, rather than degradation products (Furlong and Carpenter 1988). Additionally, high campesterol (relative to campestanol) at B16 and B17 in 2018 point to fresh delivery of diatom remains, dinoflagellates and green algae (Volkman 1986, Volkman *et al* 2008) corroborating deposition of recent material. Direct, rapid deposition of algal biomass such as the filamentous *Melosira arctica* from melting sea-ice could also contribute to the highly labile signature, especially during initial ice-out (Boetius *et al* 2013). Together, this evidence highlights the importance of labile chloropigment and organic matter fluxes to the seafloor between and including the end of ice algal production and the open water phytoplankton bloom (Fortier *et al* 2002). Earlier 2018 sea-ice loss in the Barents Sea will have also altered the timing of the spring bloom, with potentially cascading effects on mid-summer production (Gaffey *et al* 2022), likely bringing forward deposition of the most labile bloom closer to the timing of sampling.

4.3. Biogeochemical change across the Polar Front

Increases in multiple markers around station B14 point to evidence of a distinct region of productivity and changing organic matter composition deposited across the Polar Front where Arctic and Atlantic water masses converge (figure 4). Changes in organic matter across the Polar Front in the Barents Sea have previously been evidenced by changes in the signature of sedimentary pyrolysis products, pointing to distinct differences in the composition of the source of OM (e.g. fish, phytoplankton, ice-age, zooplankton) (Stevenson and Abbott 2019) and by contrasting nutrient conditions and phytoplankton community composition (Downes *et al* 2021). The transition across the Polar Front is also marked by transition in the bioturbation activity of benthic animals (Solan *et al* 2020) and their reproductive and population dynamics (Reed *et al* 2021), with potential

consequences for the character and degradation of organic matter at the seafloor. The Polar Front is a key boundary in the spring between highly productive Arctic and Atlantic waters with comparatively lower phytoplankton abundance (Makarevich *et al* 2021). High hydroxychlorophyllone, a chlorophyll transformation product at station B14 suggests that phytoplankton organic matter delivery is relatively recent, fresh and well-preserved and could additionally point to protist grazing activity (Kashiyama *et al* 2012, Tait *et al* 2015) and therefore, the presence of a productive and tightly-coupled pelagic food-chain. High 19'-hexanoyloxyfucoxanthin at B14 point to the presence of prymnesiophytes (Haberman *et al* 2003), a class of haptophyte algae and some dinoflagellates (Tangen and Björnland 1981), reinforcing the Polar Front as a zone of high productivity.

Higher productivity in 2019 at stations B13 and B14 (figures 2 and 3) close to the Polar Front also point to a larger bloom further south in the vicinity of the zone where Atlantic and Arctic water masses converge (Oziel *et al* 2016). In 2019 advection of phytoplankton cells from the Atlantic sector of the Barents Sea could have been higher, concentrating larger cells (which are more easily advected (Wassmann *et al* 2006, Font-Muñoz *et al* 2017)) around this area, stimulating production. This highlights heterogeneity in spatial and temporal variability between years.

4.4. Tracing Atlantic versus Arctic water productivity at the periphery of the Barents Sea

Geochemical markers also highlight the secondary signature of peripheral contrasting Atlantic productivity among sampled stations. For example, higher total sterols at the westerly station B03 in 2019 point to a pulse of productivity entering the shelf from the Atlantic, consistent with the direction of the North Atlantic Current into the Barents Sea, a phenomenon which has been previously associated with warming (Neukermans *et al* 2018) (figure 5(a)). Higher ratios of the microbial C_{14}, C_{15} and C_{16} iso FAMEs relative to the saturated $C_{16:0}$ FAME at stations B03 and in 2017/18 at B13 point to enhanced sedimentary bacterial activity (Perry *et al* 1979), probably reflecting greater degradation in highly reactive sediments enabled by warmer bottom temperatures and/or differences in the delivery and quality of phytoplankton to the seafloor (figure 5(b)). A slight pulse in the same indicator at the most northerly station B18 (sampled 2017) could indicate the northern signature of Atlantic water masses and the effect on sediment around the north of Svalbard. Enhanced preservation of key sterol ratios (dinosterol/dinostanol & stigmasterol/stigmastanol) (figures 5(c) and (d)) at westerly and southerly stations B03 and B13 point to unique source or productivity from the Atlantic sector, with enhanced dinosterol probably reflective of a dinoflagellate source (Boon *et al* 1979).

4.5. Implications in a changing Arctic

With a long-term trend to reduced summer sea-ice extent in the Arctic, together with an increasing likelihood of more frequent early ice-out (as in 2018 (Sumata *et al* 2022)), the future delivery of organic matter to the seafloor is likely to change, with earlier and more productive phytoplankton blooms. This will have consequences both for the benthic animals which feed on detritus at the seafloor (Solan *et al* 2020) and on the microbiology and resulting organic matter processing in sediments beneath (Stevenson *et al* 2020). This could result in increased feeding in areas of the seafloor beneath early ice-out scenarios, but reduced feeding in areas no longer proximal to ice-out scenarios, disrupting previously anticipated Arctic benthic animal phenology (Górska and Włodarska-Kowalczuk 2017). However, as the zone of most-labile organic matter moves northwards, southern sectors of the Barents Sea, areas close to the Polar Front will likely receive less phytoplankton-derived organic matter and of a less nutritious quality, impacting benthic animal activities, sedimentary microbial decomposition of organic matter and reductions in carbon storage at the seafloor.

5. Conclusions

Consistent with the wider recorded decline in Arctic sea-ice in 2018, we find marked increases in chlorophyll and carotenoid pigments and fatty acids deposited at the seafloor in the northern part of our transect in the Barents Sea, in contrast to more conventional deposition scenarios in 2017 and 2019. Importantly, our analyses indicate earlier ice-out in 2018 enabled conditions supportive of deposition of labile algal-rich organic matter to the seafloor, facilitated by post-melt phytoplankton blooms or deposition of degraded ice-attached algae directly to the sediment-water interface. The labile, highly reactive signature of this material deposited to surface sediments in 2018, confirm its recent seasonal deposition. Close relationships between satellite derived chlorophyll *a* and multiple indicators of productivity highlight the links between post-ice out pelagic algal blooms and deposition of this organic matter to the seafloor. Additionally, this study found evidence of a differing organic matter signature in the vicinity (both north and south) of the frequently observed Polar Front system in the Barents Sea, plus secondary evidence of Atlantic water mass influence in the most southerly and westerly sampling stations. Continued retreat of Arctic sea-ice, exemplified by early ice-out scenarios such as in 2018 driven by warming, together with gradual movement of the Polar Front northwards will alter the quality, abundance and position of organic matter delivery to the seafloor. This has clear consequences on benthic biology, microbial degradation of organic matter and likely changes in carbon storage at the seafloor.

Data availability statements

Sea ice cover maps (figure 1 and SI figure 1) are based on the AMSR2 ASI Sea Ice Algorithm sea ice concentration data product (https://doi.org/10.1594/PANGAEA.898399) (Spreen *et al* 2008) which is publicly available (https://seaice.uni-bremen.de/data-archive) (Remote Sensing for Polar Regions working group from the Remote Sensing department at the Institute of Environmental Physics, Universität Bremen) and is based on publicly available data from satellite GCOM-W1 (https://gportal.jaxa.jp/gpr). Sea-surface chlorophyll *a* in ice-free water maps (SI figures 9–17) use publicly available OC-CCi v5.0 data (https://climate.esa.int/en/projects/ocean-colour/news-and-events/news/ocean-colour-version-50-data-release/) and were processed by NEODAAS (NERC Earth Observation Data Acquisition and Analysis Service) (www.neodaas.ac.uk/). Geochemical seafloor data analysed for this study are included in supplementary information file 2. Temperature and salinity data (SI figure 18) from CTD profiles are compiled from Changing Arctic Ocean (CAO) cruises (2017–2019) available publicly from the British Oceanographic Data Centre (BODC) (www.bodc.ac.uk).

Author contributions

GDA and RA prepared grant application and obtained funding. MAS carried out shipboard field-work and sampling with collaborators. MAS and RA performed laboratory and numerical analyses. MAS produced plots and drafted manuscript. All authors contributed to discussion of results and final manuscript.

Additional information

Competing financial interests: The authors declare no competing financial interests. Sediment sampling was completed in the Barents Sea with appropriate permissions obtained by British Antarctic Survey, during the NERC Changing Arctic Ocean (CAO) programme (www.changing-arctic-ocean.ac.uk).

References

Airs R L, Atkinson J E and Keely B J 2001 Development and application of a high resolution liquid chromatographic method for the analysis of complex pigment distributions *J. Chromatogr.* A **917** 167–77

Airs R L and Keely B J 2000 A novel approach for sensitivity enhancement in atmospheric pressure chemical ionisation liquid chromatography/mass spectrometry of chlorophylls *Rapid Commun. Mass Spectrom.* **14** 125–8

Ardyna M, Babin M, Gosselin M, Devred E, Rainville L and Tremblay J-É 2014 Recent Arctic Ocean sea ice loss triggers novel fall phytoplankton blooms *Geophys. Res. Lett.* **41** 6207–12

Arrigo K R *et al* 2012 Massive phytoplankton blooms under Arctic sea ice *Science* **336** 1408

Barton B I, Lenn Y-D and Lique C 2018 Observed atlantification of the Barents Sea causes the Polar Front to limit the expansion of winter sea ice *J. Phys. Oceanogr.* **48** 1849–66

Belicka L L, Macdonald R W and Harvey H R 2002 Sources and transport of organic carbon to shelf, slope, and basin surface sediments of the Arctic Ocean *Deep Sea Res.* I **49** 1463–83

Belt S T, Cabedo-Sanz P, Smik L, Navarro-Rodriguez A, Berben S M P, Knies J and Husum K 2015 Identification of paleo Arctic winter sea ice limits and the marginal ice zone: optimised biomarker-based reconstructions of late Quaternary Arctic sea ice *Earth Planet. Sci. Lett.* **431** 127–39

Boetius A *et al* 2013 Export of algal biomass from the melting arctic sea ice *Science* **339** 1430–2

Boon J J, Rijpstra W I C, de Lange F, de Leeuw J W, Yoshioka M and Shimizu Y 1979 Black Sea sterol—a molecular fossil for dinoflagellate blooms *Nature* **277** 125–7

Bretones A, Nisancioglu K H, Jensen M F, Brakstad A and Yang S 2022 Transient increase in Arctic deep-water formation and ocean circulation under sea ice retreat *J. Clim.* **35** 109–24

Comiso J C 2003 Large-scale characteristics and variability of the global sea ice cover *Sea Ice: An Introduction to Its Physics, Chemistry, Biology and Geology* ed D Thomas and G S Dieckman (Blackwell Malden) pp 112–42

Comiso J C, Parkinson C L, Gersten R and Stock L 2008 Accelerated decline in the Arctic sea ice cover *Geophys. Res. Lett.* **35** 1–6

Dong K, Kvile Ø K, Stenseth N C and Stige L C 2020 Associations among temperature, sea ice and phytoplankton bloom dynamics in the Barents Sea *Mar. Ecol. Prog. Ser.* **635** 25–36

Downes P P, Goult S J, Woodward E M S, Widdicombe C E, Tait K and Dixon J L 2021 Phosphorus dynamics in the Barents Sea *Limnol. Oceanogr.* **66** S326–42

Falk-Petersen S, Mayzaud P, Kattner G and Sargent J R 2009 Lipids and life strategy of Arctic Calanus *Mar. Biol. Res.* **5** 18–39

Falk-Petersen S, Sargent J R, Henderson J, Hegseth E N, Hop H and Okolodkov Y B 1998 Lipids and fatty acids in ice algae and phytoplankton from the Marginal Ice Zone in the Barents Sea *Polar Biol.* **20** 41–47

Faust J C, Ascough P, Hilton R G, Stevenson M A, Hendry K R and März C 2023 New evidence for preservation of contemporary marine organic carbon by iron in Arctic shelf sediments *Environ. Res. Lett.* **18** 014006

Faust J C, Stevenson M A, Abbott G D, Knies J, Tessin A, Mannion I, Ford A, Hilton R G, Peakall J and März C 2020 Does Arctic warming reduce preservation of organic matter in Barents Sea sediments? *Phil. Trans. R. Soc.* A **378** 20190364

Faust J C, Tessin A, Fisher B J, Zindorf M, Papadaki S, Hendry K R, Doyle K A and März C 2021 Millennial scale persistence of organic carbon bound to iron in Arctic marine sediments *Nat. Commun.* **12** 275

Fischer A D, Moberg E A, Alexander H, Brownlee E F, Hunter-Cevera K R, Pitz K J, Rosengard S Z and Sosik H M 2014 Sixty years of Sverdrup: a retrospective of progress in the study of phytoplankton blooms *Oceanography* **27** 222–35

Font-Muñoz J S, Jordi A, Tuval I, Arrieta J, Anglès S and Basterretxea G 2017 Advection by ocean currents modifies phytoplankton size structure *J. R. Soc. Interface* **14** 20170046

Fortier M, Fortier L, Michel C and Legendre L 2002 Climatic and biological forcing of the vertical flux of biogenic particles under seasonal Arctic sea ice *Mar. Ecol. Prog. Ser.* **225** 1–16

Fossheim M, Nilssen E M and Aschan M 2006 Fish assemblages in the Barents Sea *Mar. Biol. Res.* **2** 260–9

Furlong E T and Carpenter R 1988 Pigment preservation and remineralization in oxic coastal marine sediments *Geochim. Cosmochim. Acta.* **52** 87–99

Gaffey C B, Frey K E, Cooper L W and Grebmeier J M 2022 Phytoplankton bloom stages estimated from chlorophyll pigment proportions suggest delayed summer production in low sea ice years in the northern Bering Sea *PLoS One* **17** e0267586

Górska B and Włodarska-Kowalczuk M 2017 Food and disturbance effects on Arctic benthic biomass and production size spectra *Prog. Oceanogr.* **152** 50–61

Haberman K L, Ross R M and Quetin L B 2003 Diet of the Antarctic krill (Euphausia superba Dana): II. Selective grazing in mixed phytoplankton assemblages *J. Exp. Mar. Biol. Ecol.* **283** 97–113

Holtvoeth J, Vogel H, Wagner B and Wolff G A 2010 Lipid biomarkers in Holocene and glacial sediments from ancient Lake Ohrid (Macedonia, Albania) *Biogeosciences* **7** 3473–89

Hop H and Pavlova O 2008 Distribution and biomass transport of ice amphipods in drifting sea ice around Svalbard *Deep Sea Res.* II **55** 2292–307

Ji R, Jin M and Varpe Ø 2013 Sea ice phenology and timing of primary production pulses in the Arctic Ocean *Glob. Change Biol.* **19** 734–41

Kahru M, Lee Z, Mitchell B G and Nevison C D 2016 Effects of sea ice cover on satellite-detected primary production in the Arctic Ocean *Biol. Lett.* **12** 20160223

Kashiyama Y *et al* 2012 Ubiquity and quantitative significance of detoxification catabolism of chlorophyll associated with protistan herbivory *Proc. Natl Acad. Sci.* **109** 17328–35

Kędra M *et al* 2015 Status and trends in the structure of Arctic benthic food webs *Polar Res.* **34** 23775

Loeng H 1991 Features of the physical oceanographic conditions of the Barents Sea *Polar Res.* **10** 5–18

Lundesgaard Ø, Sundfjord A, Lind S, Nilsen F and Renner A H H 2022 Import of Atlantic water and sea ice controls the ocean environment in the northern Barents Sea *Ocean Sci.* **18** 1389–418

Makarevich P R, Larionov V V, Vodopyanova V V, Bulavina A S, Ishkulova T G, Venger M P, Pastukhov I A and Vashchenko A V 2021 Phytoplankton of the Barents Sea at the polar front in spring *Oceanology* **61** 930–43

Morata N and Renaud P E 2008 Sedimentary pigments in the western Barents Sea: a reflection of pelagic–benthic coupling? *Deep Sea Res.* II **55** 2381–9

Neukermans G, Oziel L and Babin M 2018 Increased intrusion of warming Atlantic water leads to rapid expansion of temperate phytoplankton in the Arctic *Glob. Change Biol.* **24** 2545–53

Notz D and Stroeve J 2016 Observed Arctic sea-ice loss directly follows anthropogenic CO_2 emission *Science* **354** 747–50

Onarheim I H and Årthun M 2017 Toward an ice-free Barents Sea *Geophys. Res. Lett.* **44** 8387–95

Orlova E L, Dolgov A V, Renaud P E, Greenacre M, Halsband C and Ivshin V A 2015 Climatic and ecological drivers of euphausiid community structure vary spatially in the Barents Sea: relationships from a long time series (1952–2009) *Front. Mar. Sci.* **1** 74

Oziel L, Neukermans G, Ardyna M, Lancelot C, Tison J-L, Wassmann P, Sirven J, Ruiz-Pino D and Gascard J-C 2017 Role for Atlantic inflows and sea ice loss on shifting phytoplankton blooms in the Barents Sea *J. Geophys. Res. Oceans* **122** 5121–39

Oziel L, Sirven J and Gascard J C 2016 The Barents Sea frontal zones and water masses variability (1980–2011) *Ocean Sci.* **12** 169–84

Pavlov V, Pavlova O and Korsnes R 2004 Sea ice fluxes and drift trajectories from potential pollution sources, computed with a statistical sea ice model of the Arctic Ocean *J. Mar. Syst.* **48** 133–57

Pearson E J, Farrimond P and Juggins S 2007 Lipid geochemistry of lake sediments from semi-arid Spain: relationships with source inputs and environmental factors *Org. Geochem.* **38** 1169–95

Perry G J, Volkman J K, Johns R B and Bavor H J 1979 Fatty acids of bacterial origin in contemporary marine sediments *Geochim. Cosmochim. Acta.* **43** 1715–25

Post E 2017 Implications of earlier sea ice melt for phenological cascades in arctic marine food webs *Food Webs* **13** 60–66

Ravenschlag K, Sahm K, Pernthaler J and Amann R 1999 High bacterial diversity in permanently cold marine sediments *Appl. Environ. Microbiol.* **65** 3982–9

Reed A J, Godbold J A, Solan M and Grange L J 2021 Reproductive traits and population dynamics of benthic invertebrates indicate episodic recruitment patterns across an Arctic polar front *Ecol. Evol.* **11** 6900–12

Renaud P E, Morata N, Carroll M L, Denisenko S G and Reigstad M 2008 Pelagic–benthic coupling in the western Barents Sea: processes and time scales *Deep Sea Res.* II **55** 2372–80

Renaud P E, Riedel A, Michel C, Morata N, Gosselin M, Juul-Pedersen T and Chiuchiolo A 2007 Seasonal variation in benthic community oxygen demand: a response to an ice algal bloom in the Beaufort Sea, Canadian Arctic? *J. Mar. Syst.* **67** 1–12

Sathyendranath S *et al* 2019 An ocean-colour time series for use in climate studies: the experience of the ocean-colour climate change initiative (OC-CCI) *Sensors* **19** 4285

Schubert C J and Stein R 1997 Lipid distribution in surface sediments from the eastern central Arctic Ocean *Mar. Geol.* **138** 11–25

Serreze M C, Maslanik J A, Scambos T A, Fetterer F, Stroeve J, Knowles K, Fowler C, Drobot S, Barry R G and Haran T M 2003 A record minimum arctic sea ice extent and area in 2002 *Geophys. Res. Lett.* **30** 1–4

Siddon E C, Zador S G and Hunt G L 2020 Ecological responses to climate perturbations and minimal sea ice in the northern Bering Sea *Deep Sea Res.* II **181–2** 104914

Smedsrud L H *et al* 2013 The role of the Barents Sea in the Arctic climate system *Rev. Geophys.* **51** 415–49

Solan M, Ward E R, Wood C L, Reed A J, Grange L J and Godbold J A 2020 Climate driven benthic invertebrate activity and biogeochemical functioning across the Barents Sea polar front *Phil. Trans. R. Soc. A* **378** 20190365

Spreen G, Kaleschke L and Heygster G 2008 Sea ice remote sensing using AMSR-E 89-GHz channels *J. Geophys. Res. Oceans* **113** 1–14

Stabeno P J and Bell S W 2019 Extreme conditions in the Bering Sea (2017–2018): record-breaking low sea-ice extent *Geophys. Res. Lett.* **46** 8952–9

Stevenson M A *et al* 2020 Transformation of organic matter in a Barents Sea sediment profile: coupled geochemical and microbiological processes *Phil. Trans. R. Soc. A* **378** 20200223

Stevenson M A and Abbott G D 2019 Exploring the composition of macromolecular organic matter in Arctic Ocean sediments under a changing sea ice gradient *J. Anal. Appl. Pyrolysis.* **140** 102–11

Stocker T F, Qin D, Plattner G-K, Tignor M M, Allen S K, Boschung J, Nauels A, Xia Y, Bex V and Midgley P M 2014 Climate change 2013: the physical science basis. Contribution of working group I to the fifth assessment report of IPCC the intergovernmental panel on climate change

Strass V H and Nöthig E M 1996 Seasonal shifts in ice edge phytoplankton blooms in the Barents Sea related to the water column stability *Polar Biol.* **16** 409–22

Stroeve J C, Kattsov V, Barrett A, Serreze M, Pavlova T, Holland M and Meier W N 2012 Trends in Arctic sea ice extent from CMIP5, CMIP3 and observations *Geophys. Res. Lett.* **39** 1–7

Sumata H, de Steur L, Gerland S, Divine D V and Pavlova O 2022 Unprecedented decline of Arctic sea ice outflow in 2018 *Nat. Commun.* **13** 1747

Sundfjord A, Fer I, Kasajima Y and Svendsen H 2007 Observations of turbulent mixing and hydrography in the marginal ice zone of the Barents Sea *J. Geophys. Res. Oceans* **112** 1–23

Syvertsen E E 1991 Ice algae in the Barents Sea: types of assemblages, origin, fate and role in the ice-edge phytoplankton bloom *Polar Res.* **10** 277–88

Tait K, Airs R L, Widdicombe C E, Tarran G A, Jones M R and Widdicombe S 2015 Dynamic responses of the benthic bacterial community at the Western English Channel observatory site L4 are driven by deposition of fresh phytodetritus *Prog. Oceanogr.* **137** 546–58

Tamelander T, Reigstad M, Hop H and Ratkova T 2009 Ice algal assemblages and vertical export of organic matter from sea ice in the Barents Sea and Nansen Basin (Arctic Ocean) *Polar Biol.* **32** 1261

Tamelander T, Renaud P E, Hop H, Carroll M L, Ambrose W G Jr and Hobson K A 2006 Trophic relationships and pelagic–benthic coupling during summer in the Barents Sea Marginal Ice Zone, revealed by stable carbon and nitrogen isotope measurements *Mar. Ecol. Prog. Ser.* **310** 33–46

Tangen K and Björnland T 1981 Observations on pigments and morphology of gyrodinium aureolum Hulburt, a marine dinoflagellate containing 19′-hexanoyloxyfucoxanthin as the main carotenoid *J. Plankton Res.* **3** 389–401

Vinje T and Kvambekk Å S 1991 Barents Sea drift ice characteristics *Polar Res.* **10** 59–68

Volkman J K 1986 A review of sterol markers for marine and terrigenous organic matter *Org. Geochem.* **9** 83–99

Volkman J K, Revill A T, Holdsworth D G and Fredericks D 2008 Organic matter sources in an enclosed coastal inlet assessed using lipid biomarkers and stable isotopes *Org. Geochem.* **39** 689–710

Wadhams P 2000 Ice in the ocean Gordon and Breach Science Publishers London, England

Walker J S, Squier A H, Hodgson D A and Keely B J 2002 Origin and significance of 132-hydroxychlorophyll derivatives in sediments *Org. Geochem.* **33** 1667–74

Ward J P J, Hendry K R, Arndt S, Faust J C, Freitas F S, Henley S F, Krause J W, März C, Tessin A C and Airs R L 2022 Benthic silicon cycling in the Arctic Barents Sea: a reaction–transport model study *Biogeosciences* **19** 3445–67

Wassmann P *et al* 2006 Food webs and carbon flux in the Barents Sea *Prog. Oceanogr.* **71** 232–87